Assessment of the feasibility of the use of conductive polymers in the fabrication of ion mobility spectrometers

ASSESSMENT OF THE FEASIBILITY OF USING CONDUCTIVE POLYMERS IN THE FABRICATION OF ION MOBILITY SPECTROMETERS.

Theodoros Koimtzis[1], Nick J. Goddard[2], Ian Wilson[3], and C.L. Paul Thomas[1*].

1. *Centre for Analytical Science, Department of Chemistry, Loughborough University, Leicestershire, LE11 3TU, UK.*
2. *CEAS, The University of Manchester, 131 Princess Street, Manchester, M1 7DN, UK.*
3. *AstraZeneca, Alderley Park, Cheshire, SK10 4TG, UK.*

* Corresponding author:

Professor C. L. Paul Thomas,
Centre for Analytical Science
Department of Chemistry,
Loughborough University,
Leicestershire,
LE11 3TU
Tel: +44 (0)1509 222549
Fax: +44 (0)1509 223925

Email: C.L.P.Thomas@lboro.ac.uk

Abstract

The development of a ion mobility spectrometer with an injection molded plastic drift tube made from carbon-loaded Nylon and the cyclo-olefinpolymer Zeonex^{TM}, is described. Thermogravimetric assessment combined with headspace analysis by ion mobility spectrometry and gas chromatography-mass spectrometry indicated that Zeonex^{TM} encapsulated carbon-loaded nylon could be used to fabricate a snap-together injection molded stacked ring drift tube, 4.25 cm long that could be substituted for a conventional wire-wound heated ceramic drift tube of the same length into a high temperature ion mobility spectrometer. Temperature stability experiments indicated that such a combination of polymers produced stable water–based reactant ion peaks $[(H_2O)_nH]^+$ up to a temperature of approximately 50°C. Above this temperature ammonia appeared to outgassed resulting in the production of $[(H_2O)_n(NH_4)_mH]^+$ type species before, at higher temperatures, the release of oligomeric entities suppressed resolved ion responses. Surface charging effects were also observed and over a period of continuous operation of 4 hr these caused suppression of the signal intensity (1.11 V to 0.954 V) and an apparent mobility shift in the observed responses (K_0 = 1.86 cm^2 V^{-1} s^{-1} to K_0 = 1.90 cm^2 V^{-1} s^{-1}.) Substituting Nylon, a polymer with a significantly lower surface resistivity, for the Zeonex demonstrated how surface charging phenomena could be managed though control of surface resistivity in future polymer formulations. The device was challenged successfully with test atmospheres of hexan-1-ol (K_0 = 1.66 cm^2 V^{-1} s^{-1} (monomer) and 1.32 cm^2 V^{-1} s^{-1}(dimer)) and dimethylmethyl phosphonate (K_0 = 1.70 cm^2 V^{-1} s^{-1} (monomer) and 1.44 cm^2 V^{-1} s^{-1}(dimer)). The potential advantages of developing polymeric systems using more advanced polymer formulations are discussed.

Introduction

Ion mobility techniques continue to be developed and refined for a wide variety of applications. Most notably ion mobility spectrometry (IMS) is used widely in security/military applications[1], and other recent methodologies would include the use of IMS for: diagnostic[2]; biomedical discovery[3, 4]; food quality and environmental[5] screening applications[6, 7]. Another vitally important aspect of IMS is the continuing development of IMS-MS systems and applications, and a recent review provides a useful and informed overview of this area[8].

The construction of conventional stacked-ring ion mobility drift tubes is a skilled and time-consuming process[1], and miniaturization of such designs is problematic for the field defining electrode geometries are constrained by the manufacturing techniques available to build them. So, although miniature ion mobility spectrometers have been demonstrated, the ultimate sizes of such devices are limited until: better fabrication methods; more effective management of electric field homogeneity; higher levels of electrical shielding; suppression of electric field fringing phenomena in small volumes; and, elimination of charging of the inner surfaces of miniaturized drift tubes have all been addressed. Meanwhile, the established processes and materials are expensive to implement, and will continue to block the development of instrument design and the associated spatial geometries of the internal elements of the instrument.

Alternative approaches to a stacked ring design have been developed with ceramic or glass drift tubes fitted with flexible conducting electrodes wrapped around the outside [1, 9]. Coated ceramics were proposed early on the development of IMS systems for security/military applications[10] and latterly, resistive glass[11, 12] and conductive ink[13] have been proposed as alternative approaches for making drift tubes. Such approaches illustrate how different materials may be exploited to develop new approaches to IMS instrument construction, design and development.

Plastic and conductive polymers have been used effectively in the development of other instrument systems; most notably in optically-based instruments[14]. Detectors based on conducting polymers[15] demonstrated the detection and management of ionic species with plastic components. The electrochemical theme was amplified and developed with the description of hybrid micro-fluidic sensors that combined the

polymer fabrication techniques of screen printing and injection molding to produce electrochemical and electrochemiluminescent transduction systems. Injection molded approaches have also been demonstrated in the isotachophoresis of anionic, alkaline ions, transition ions and lanthanide ions[16]. More recently, miniaturized polymeric isotachophoresis devices have been demonstrated for DNA extraction from whole blood[17]. Success in the demonstration of polymeric instruments for the separation and detection of ions in liquid phases raises questions about the feasibility of polymeric and injection molding approaches to IMS.

Polymer-based fabrication approaches would reduce the cost, substantially, of producing IMS instrumentation. Furthermore, injection molding approaches using electrically conductive, insulating and static dissipative polymers may be envisaged as a route to develop miniaturized IMS systems, and simplify the drift tube design and manufacture process. The possibility of highly automated manufacture and reduction of materials cost has the potential to place IMS-based methods into new conceptual frameworks. Finally, injection molding approaches enable new internal structures for drift tubes to be created and explored. If adoption of injection molding approaches were feasible then designs and approaches not realizable by established construction methods, but possible using liquid plastics within molds would be accessible.

This study sought to demonstrate the use of plastic in the construction of a drift tube for an ion mobility spectrometer and to identify the developmental and technical challenges that need to be addressed in the development of fully plastic IMS systems.

Experimental

Polymers

Nylon and carbon-loaded nylon were obtained from LNP Engineering Plastics Ltd, Solihull, UK. Zeonex™ and Zeonor™ were supplied by Nippon Zeon Ltd, Cardiff, UK., and carbon-loaded polystyrene was supplied by Northern Industrial Plastics Ltd, Chadderton, UK. The degassing and melting point temperatures are summarized in Table 1

Polymer Characterization and Selection

The polymers were tested to determine which of these plastics provided the most likely combination of compatible materials. Gravimetric analysis during thermal

conditioning, followed by headspace analysis by IMS and gas chromatography-mass spectrometry (GC-MS) were used to assess the candidate materials.

Gravimetric analysis during thermal conditioning at 90^{o}C over 85 hr was performed on 3 g samples of the polymers in their granulated form, after which the polymers were allowed to re-equilibrate with ambient atmosphere (1069 $ppm_{(V)}$<[H_2O]<1438 $ppm_{(v)}$) for 7 days. The masses of the polymer samples were recorded throughout this period, see Figure 1

At 90^{o}C all the polymers lost mass rapidly for up to the first 11 hr. Carbon-loaded polystyrene, Zeanor and Zeonex all lost approximately 0.1 % of their mass followed by some additional mass loss continuing for a further 24 hr. No further mass loss was observed after this. At the end of thermal conditioning these polymers re-equilibrated with ambient air rapidly, following first pseudo first-order kinetics, stabilizing within 15 minutes.

Carbon-loaded nylon lost 0.5 % of its mass in the first 11 hrs and then stabilized. This material re-equilibrated more slowly than the first three regaining its initial mass after 7 days. Nylon, however, underwent irreversible mass loss on heating to 90 °C losing ca. 1.75% of its mass in the first 11 hr, and then continuing to lose a further 0.1% over the next 69 hr. Over the course of the 7 day re-equilibration period Nylon regained mass but did not stabilize.

The observations for Zeanor, Zeonex, carbon-loaded polystyrene and carbon-loaded nylon were consistent with the release and re-absorption of water. Nylon's mass-loss data were indicative of thermal decomposition followed by re-absorption of water.

Purge and trap headspace analysis was performed on samples (3g) in granular form by purging a headspace vial, containing the sample, connected to an adsorbent trap (Markes international Ltd, Gwaun Elai Medi Science Campus Llantrisant RCT, CF72 8XL UK, 150 mg Tenax Ta) by a deactivated capillary, with nitrogen. Trapped volatiles were recovered and analyzed with a two-stage thermal desorption procedure. (Markes International Ltd. Unity Thermal Desorber), gas chromatography mass spectrometry (60 m long, 0.25 mm diameter, 0.25 µm film thickness with a 5% phenyl, 95 % methyl polysiloxane stationary phase; Agilent UK, DB-5MS). The mass spectrometer was an ion trap (Varian, 2200, 2700 Mitchell Dr Walnut Creek, CA) see Table 2.

Figure 2 shows example chromatograms from these tests, and all polymers released a range of oligomeric compounds in their unconditioned state. However the extent of this release was not significant with Zeonex, Zeonor and polystyrene; levels were synonymous with low ppb(v) concentrations in the headspace vial. Nylon, in contrast, gave a more complex profile with levels up to 50 times higher than the other materials.

The final test characterized the headspace vapors from the polymers by IMS. Samples of the granular polymers (3 g) were placed into a headspace vial, maintained at a constant temperature (18 °C to 19.5°C) that was connected by a sheath-flow inlet to an ion mobility spectrometer (HiTIMS, Smiths Detection, Watford, Hertfordshire, UK, Formally Graseby Dynamics)[18], see Table 3 for a summary of the experimental conditions, and Figure 3 for example mobility spectra.

The only responses observed were in the reactant ion peak region; no other product ions were observed up to a drift time of 45 ms. Zeonor, Zeonex and conductive polystyrene produced broadly similar effects with the predominant reactant ion (assigned as $[(H_2O)_nH]^+$) reducing in intensity and broadening . An additional higher mobility feature was also observed (attributed as $[(H_2O)_n(NH_4)_m\ H]^+$). The reduced mobility of the water-based reactant ion peak also shifted to lower mobility, relative to the reference signal. These observations were consistent with the gravimetric data. They are indicative of water release from the polymer resulting in a shift of the hydration envelope to larger numbers of water molecules within the reactant ion clusters and the release of trace levels of ammonia. Nylon and conductive nylon caused marked shifts of the water-based reactant ion peaks to lower mobilities accompanied by the development of significant ammonia-based features. With a loss of resolution and intensity in the reactant ion peak, all of which was consistent with the gravimetric data.

The headspace IMS tests were repeated after conditioning the polymers by heating to 90 °C in a vacuum oven (100 Pa) and leaving overnight > 12 hr, see Figure 3. The responses were entirely consistent with reductions in the levels of water and ammonia. Indeed only carbon loaded polystyrene was observed to still generate an ammonia-related response after conditioning. Table 4 summarizes the mobility data from these tests.

The observations from the polymer characterization study emphasized the need for conditioning polymers before their use. Conductive nylon has a higher temperature stability than conductive polystyrene, however the levels of out-gassing meant the drift tube design had to provide encapsulation of the carbon-loaded nylon field defining electrodes with Zeonex; chosen for its higher thermal stability over Zeonor.

Design

Finite element modelling software (Comsol Multiphysics Ver 3.2) was used to optimize the design of the polymeric drift tube. The starting point was an evaluation of the HiTIMS system; that was to be modified to accept an injection molded drift tube. The wires that supply voltages to the field defining electrodes were also included in the model and as a consequence the routing and connections associated with power supplies and field defining electrodes were identified as important in establishing a homogeneous electric field in the drift tube. Radial connections were found to generate the most homogeneous electric fields and the final design eliminated wires from within the electrical shielding of the drift tube, see Figure 4.

The drift tube was based on a stack of interleaved polymer disks that snapped together with alternate conducting polymer disks and insulating polymer spacers. The field defining electrodes were made from conducting nylon and the spacing disks were made from Zeonex and encapsulated the conducting nylon electrodes suppressing released vapors. The number of field defining electrodes and the spacing between them was based on the wire wound ceramic drift tube that they were to replace. The field defining electrodes were designed to receive a snap-on electrical connector, and Figure 5 shows an exploded view of the design with detail of the final drift tube.

An accurate three-dimensional mechanical model of the injection molding parts was developed in (Desktop Inventor run on a PC operating under a Windows XP OS) The model included the relevant parts of the injection molder (Babyplast 6/10 machine) a pair of molds, and the resulting molded part, see Figure 5. The designs for the individual mold parts were exported into machine control software (Edgecam, Orbital House, Moat Way, Ashford, Kent, TN24 0TT, UK.) that produced the CNC control codes for micro-machining the aluminium parts. The micro-machining was performed using a CAT3D-M6 micro-machining centre (Datron Electronic GmbH, Mühltal, Germany). The finished molds were washed with water and sonicated in a cleaning

solution (Decon 90 in de-ionised water) followed by methanol, each for 15 min, before conditioning in a vacuum oven at 120°C for two hours.

Instrumentation

Drift tube. The conducting nylon and Zeonex polymers in their granulated form were conditioned immediately prior to use (90°C, 100 Pa >12 hr), and loaded into a Babyplast 6/10. This injection molder is for the fabrication of small plastic parts and is suitable for prototype fabrication with "easy-to-handle" polymers. The injection molding parameters were empirically optimized and are summarized in Table 5. Once set-up, field defining electrodes were produced at a rate of up to 360 parts per hour.

Once cool the polymeric parts were removed from their spree and sonicated for 30 min in a cleaning solution (Decon 90), before rinsing with deionised water and drying under vacuum for 10 hours. The stacked electrodes were then snapped together and fitted between the inlet and detector stages of a high temperature ion mobility spectrometer (Smiths Detection), see Figure 5, a procedure that took no more than 5 minutes. The modified ion mobility spectrometer with the plastic drift tube was then inserted into temperature regulated housing.

Ion Mobility spectrometer: The wire-wrapped ceramic drift tube from a high temperature ion mobility spectrometer (HiTIMS, Graseby Dynamics, now Smiths Detection, Park Road, Bushy, Watford, Hertfordshire WD23 2BW.) was replaced with the injection molded drift tube. The instrument was operated through a virtual instrument developed in LabVIEW (National Instruments Corporation (UK), Measurement House, Newbury Business Park, London Road, Newbury, Berkshire, RG14 2PS UK), installed on a desktop computer. (PC 800Mhz processor, 512MB RAM, Windows 2000, fitted with a PCI-6024E multifunction card (National Instruments)). The 510 pin design printed circuit board provided an electrical isolation barrier (1.5kV) for all digital and analogue channels protecting the interface electronics as well as the data acquisition hardware and PC from the high voltages within the IMS system. Heater power and shutter-grid voltages were supplied from isolated circuits to suppress noise coupling into the analogue lines associated with the detector interface. The high voltage supply to the field defining electrodes was delivered from a 25W, high-voltage PSU unit (Thurlby Thandar Instruments Ltd. Glebe Road, Huntingdon, Cambridgeshire PE29 7DR, UK).

Experimental Tests

Temperature effects.

The effect of temperature on the polymeric drift tube was studied by monitoring the reactant ion peak during temperature programmed experiments which heated the drift tube to 80°C and then allowed it to cool to 24°C. A spectrum from 50 averaged scans was obtained at every 1°C step. The data were processed in LabviewTM and rendered into three dimensional surfaces showing drift time intensities against temperature, Figure 6.

Stability

The stability of the polymer drift tubes were evaluated by continuously monitoring the reactant ion peak at ambient temperature with a drift flow of 250 cm^3 min^{-1} with a shutter pulse duration of 300 μs for up to 4 hr, Figure 7.

Comparison of responses

Two gravimetrically calibrated permeation sources, one containing hexan-1-ol, the other dimethylmethylphosphonate, were fitted into a test atmosphere generator that delivered 2 ppm(v) at 10 cm^3 min^{-1} to a sheath flow inlet at the IMS (sheath flow 50 cm^3min^{-1} and drift gas flow 150 cm^3min^{-1}). The sheath flow inlet was adjusted to provide clearly resolved ion mobility spectra The data acquisition parameters were 60 averaged spectra collected at a rate of 10 kHz with a shutter pulse duration of 300 μs. Drift times were measured from the ion gate closure, Figure 8.

Results.

The effect of Temperature

Figure 6 is a false color image of the temperature response surface recorded during the temperature programming experiment. To begin with the reactant ion peak shifted to higher mobility (lower drift time), indicated by the letter “A” with increasing temperature. This was due to the reduction in the size of the hydration envelope of the reactant ion as it shifted to smaller clusters. Superimposed onto this shift to increasing mobility was the likely emergence of an ammonium ion signal, which by 50 °C appeared to have sequested most of the charge from the original reactant ion peak; leaving a residue water-based signal (see B on the enlarged inserts in Figure 6). From

about 50°C upwards the mixed ammonium/water peak diminished into a complicated and difficult to resolve set of disparate features. Indeed, increasing the temperature still further resulted in the emergence of out-gassed and thermal breakdown compounds that yielded a complicated and low intensity set of superimposed ion mobility peaks (see C in Figure 6) with a concomitant suppression of the ammonium/water peak.

Stability.

The results of the stability tests enabled drying, surface charging and out-gassing phenomena to be studied. Figure 7 (Top) shows how encapsulation of the field defining electrodes with Zeonex resulted in a single, water-based, reactant ion peak which increased in mobility over the first 35 min; K_0 = 1.86 $cm^2 V^{-1} s^{-1}$ to K_0 = 1.90 $cm^2 V^{-1} s^{-1}$. The intensity of this reactant ion peak also reduced during this time from 1.11 V to 0.954 V. After 35 min the mobility started to reduce, so that after 4 hr K_0 = 1.81 $cm^2 V^{-1} s^{-1}$. The intensity of the peak also continued to decrease; 0.85 V after 4 hr. The shift in drift time and reduction in intensity were reversible and switching the instrument off resulted in the system regaining its sensitivity and the mobility returning to a value of 1.88 $cm^2 V^{-1} s^{-1}$.

The increase in the reduced mobility observed during the first 35 min was consistent with the drying phenomena observed during the polymer evaluation tests. The loss of sensitivity throughout the test, and the subsequent observed decrease in mobility were attributed to the accumulation of charge on the internal Zeonex surface of the drift tube. (The surface resistivity of Zeonex is $1x10^{16}$ **Ω)**

This proposition was tested by substituting the Zeonex spacers with ones made from Nylon. (Nylon has a surface resistivity 10^4 times lower than Zeonex at $1x10^{12}$ **Ω** and it is more hydrophilic, so adsorbed water would reduce the resistivity still further. Nylon, however, releases ammonia and the mobility spectrum was anticipated to contain a significant ammonia component.) The resultant ion mobility spectrum did indeed contain an ammonium ion peak as-well-as the water-based reactant ion peak. On start-up the mobility of the water-based reactant ion peak increased over 20 minutes: K_o = 1.80 $cm^2 V^{-1} s^{-1}$ to K_0 = 1.87 $cm^2 V^{-1} s^{-1}$. Likewise the ammonium ion peak mobility also increased from K_o = 1.92 $cm^2 V^{-1} s^{-1}$ to K_0 = 1.99 $cm^2 V^{-1} s^{-1}$. After this time the drift times of the two peaks were stable over the next four hours.

During this comparison experiment the intensity of the water-based reactant ion peak reduced from 0.71 V at the start of the run to 0.68 V after 20 min and attained 0.60 V after 4 hr. The intensity of the ammonium ion based peak increased as the water-peak decreased; starting at 0.51 V on switch-on and increasing to 0.53 V after 20 min. After 4 hr the intensity had increased further, to 0.58 V.

The initial increase in mobility was consistent with the drying phenomena observed during the polymer evaluation tests. Nylon releases ammonia and the increase of the ammonium ion based response in the Nylon encapsulated electrodes was not unexpected. The reduction in mobility accompanied by a loss in sensitivity observed with the Zeonex spacers was not observed; consistent with the suppression of the suspected surface charging phenomenon.

Response to chemical challenges.

Figure 8 presents example spectra obtained from test atmospheres of dimethylmethylphosphonate and hexan-1-ol. The spectra were obtained at 22 °C and the reduced mobilities of the ions observed agreed with those reported previously [19]. These data were collected using drift tubes that had been conditioned and stabilized in the instrument with drift gas flowing continuously through them. Before use the shutter grids had been shut to allow surface charge on the inner walls of the drift tube to dissipate. The responses were essentially the same as those observed using the wire wound ceramic drift tube of the HiTIMS; albeit with a slight reduction in sensitivity, thought to be due to be due to imperfect alignment between the drift tube and the gating electrodes and/or the shielding grid and gating detector assembly. After prolonged use, signal artifacts were observed and these were attributed to adsorption of neutral species onto the interior surfaces of the drift tube.

Summary

These data demonstrate, for the first time, the possibility of constructing an ion mobility spectrometer's drift tube from plastic components at a fraction of the cost of currently used approaches. Nevertheless, there are still challenges associated with the formulation of the most effective polymers for this type of application. The polymers used in this study were selected for their compatibility with the prototyping facilities available to the researchers. More sophisticated injection molding systems enable

temperature and pressure programming with more demanding polymer formulations, such as PEEK and PTFE. Using temperature and pressure programmed injection molding systems will also enable the optimization of the fabrication process parameters to generate homogeneous bulk conductivity within the polymer matrix on cooling. This is a non-trivial challenge for differential cooling and pressure gradients within the mold introduce heterogeneity into the cast components that result in non-linear voltage gradients across the material. Success here will enable the use of single element field defining electrodes in designs informed by the conducting glass systems and planar designs noted previously[1,2, 13].

This study also sought to identify and prioritize the technical and material science challenges that accompany a move towards polymer-based ion mobility spectrometers. Three priorities have been highlighted during the current study: out-gassing/thermal stability; surface resistivity; and, conditioning of polymer components before and after injection molding. The adoption of more thermally-stable polymers, such as PEEK and PTFE, is anticipated to extend the temperature range over which polymeric drift tubes may be used and the thermal conditioning regimes that they may be subjected to. It was no surprise to observe the importance of surface charging effects in delivering a stable and sensitive response with polymeric drift tubes. Unless charge on the surfaces of the drift-tube can be dissipated the resultant system will be difficult to operate and validate. Incorporating a static dissipative polymer component is a logical first step in this regard.

The next-steps in this research programme then are the creation, or adoption, of a polymeric formulation with a low-water content (to inhibit the release of humidity into the drift gas flow), but at the same time with slightly static dissipative attributes sufficient to provide a rate of dissipation higher than the rate of charge accumulation on the inner walls of the drift tube. As observed above, adopting injection molding approaches to drift tube designs also allows the exploration of more complex field defining designs, not feasible using established construction methods, and this is also a logical continuation of this work.

Acknowledgements

The work described in this paper was supported by a grant from AstraZeneca and took place as part of the National Initiative on Ion Mobility Spectrometry run at the former

Department of Instrument and Analytical Science at UMIST and Nottingham Trent University with support from Waters Instruments, GlaxoSmithKline and AstraZeneca.

References

(1) Eiceman G.A. and Karpas Z., "Ion mobility Spectrometry", CRC Press ISBN-10: 0849322472, **2005**.

(2) Karpas, Z.; Chaim, W.; Gdalevsky, R.; Tilman, B.; Lorber, A. *Anal. Chim. Acta*, **2002**, 474 115-123 .

(3) Westhoff, M.; Litterst, P.; Freitag, L.; Baumbach, J.I. *J. Physiology and Pharmacology*, **2007**, 58, 739-751.

(4) Vautz, W.; Baumbach, J. I. *Int. J. Ion Mob. Spec*. **2008** 11 35-41.

(5) Kanu, A. B.; Hill, H. H. Jr.; Gribb M. M.; Walters, R. N. *J. Environ. Monit.* **2007**, 9, 51-60.

(6) Karpas, Z.; Tilman, B.; Gdalevsky, R.; Lorber, A. *Anal. Chim. Acta*, **2002,** 463, 155-163.

(7) Awan, M. A.; Fleet I.; Thomas, C.L.P. *Anal. Chim. Acta*, **2008**, 611, 226-232.

(8) Kanu, A. B.; Dwivedi, P.; Tam, M.; Matz, L.; Hill, H. H. Jr., *J. Mass Spec*. **2008**, 43, 1-22.

(9) Yoon, K. W.; Hwang, K. W. W.; Lim, H. J.; Choi, S. K.; Kim, H. S. "Ion Mobility Spectrometer flexible Printed Circuit Board and Method for Manufacturing thereof". US Patent, 5834771 Nov 10 **1998**.

(10) Carrico, J. P.; Sickenberger, D. W.; Spangler, G.E.; Vora, K. N. *J. Physics E: Scientific Instruments*, **1983,** 16, 1058-1062.

(11) Laprade, B.; "Use of Conductive glass tubes to create electric fields in ion mobility spectrometers" US Patent, 7,081,618, **2006**.

(12) Kwasnik, M.; Fuhrer, K.; Gonin, M.; Barbeau, K.; Fernández, F. M. *Anal. Chem*., **2007,** 79, 7782-7791.

(13) Eiceman, G. A.; Schmidt, H.; Rodriguez, J. E.; White, C. R.; Krylov, E. V.; Stone, J. A. *Inst. Sci. and Tech*., **2007,** 35, 365-383.

(14) Narayanaswamy, R.; Wolfbeis O.S.; (eds.) "Optical Sensors: Industrial, Environmental and Diagnostic Applications"**.** Publ. Springer, Heidleberg, ISBN 3-540-40886-X, **2004**.

(15) Mylonakis, A.; Economou, A.; Fielden, P. R.; Goddard, N. J.; Voulgaropoulos, A., *Electroanalysis* , **2004,** 16, 524-531.

(16) Baldock, S. J.; Fielden, P. R.; Goddard, N. J.; Prest, J. E.; Brown, B. J. T., *J. Chromatogr. A*, **2003**, 990, 11-22.

(17) Prest, J. E.; Baldock, S. J.; Day, P. J. R.; Fielden, P. R.; Goddard, N. J.; Treves-Brown, B. J., *J. Chromatogr. A*, **2007,** 1156, 154-159.

(18) Young, D.; Thomas, C. L. P.; Breach, J.; Brittain A. H.; Eiceman, G. A., *Anal. Chim. Acta*, **1999,** 381, 69-83.

(19) Shumate, C.; St. Louis, R. H.; Hill, H. H. Jr., *J Chromatogr*. **1986,** 373, 141-173.

FIGURES

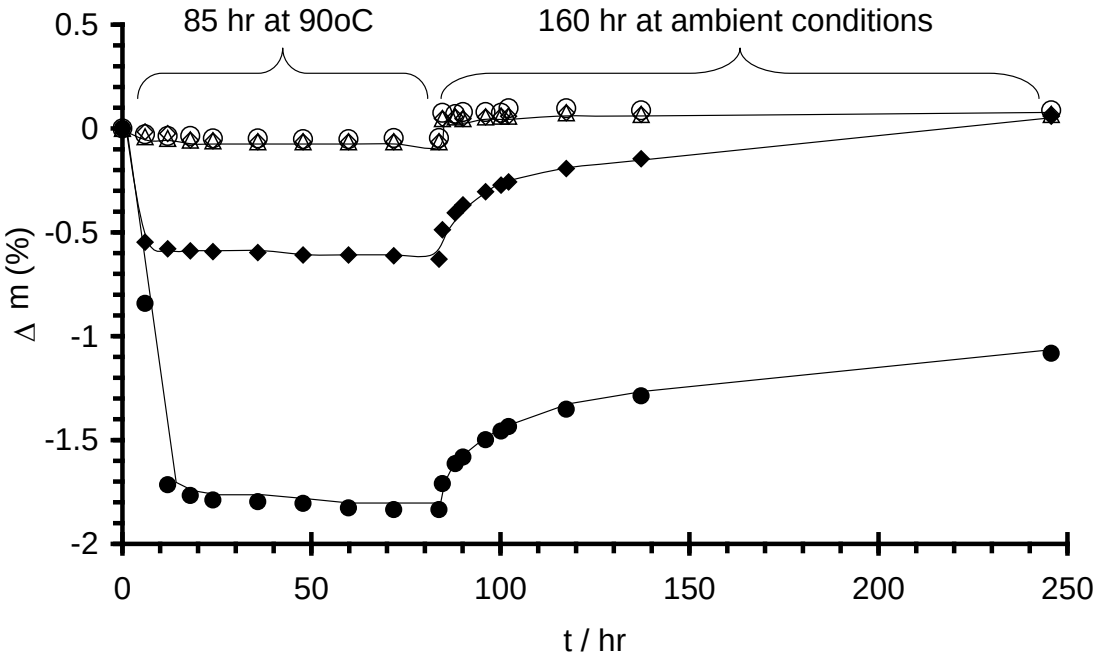

Figure 1. The results from the thermal gravimetric study of the polymers evaluated for use in this study. The upper trace of superimposed circles, diamonds and triangles was generated from the mass loss data of carbon loaded polystyrene, Zeanor and Zeonex respectively. The middle trace of solid diamonds shows the behaviour of carbon loaded nylon and the lower trace, solid circles, represents the observed mass-loss from the nylon sample.

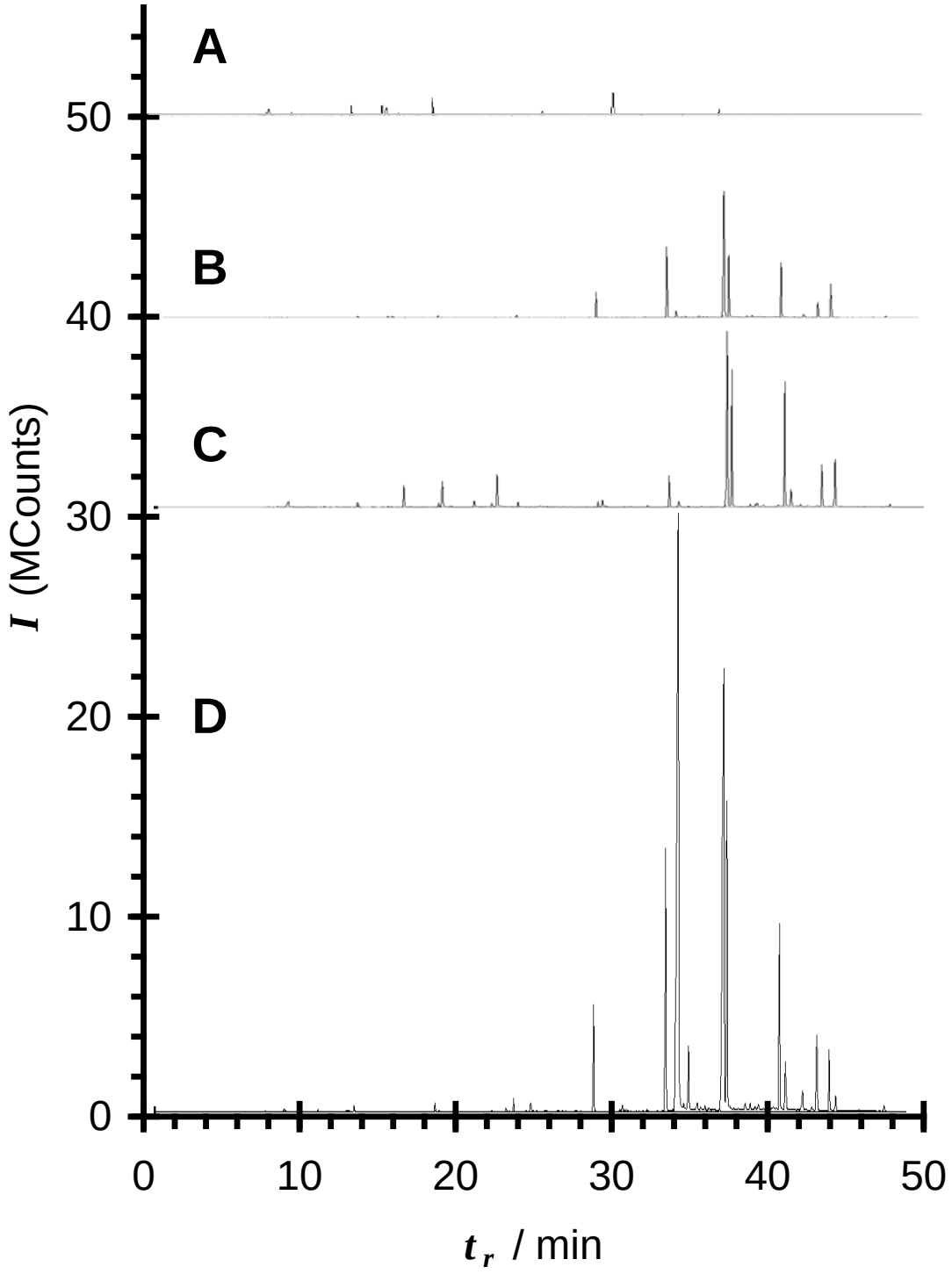

Figure 2 Examples of dynamic headspace analysis of unconditioned polymer materials by GC-MS. These total ion chromatograms show the intensity and extend of outgassed oligomer materials from: A; Zeonor, B: Zeonex; C: Polystyrene and D Nylon. The levels of outgased materials from the polystyrene, Zeonor and Zeonex materials are consistent with low ppb(v) concentrations. Nylon, in contrast, had 1 to 2 orders of magnitude more concentrated impurities associated with it.

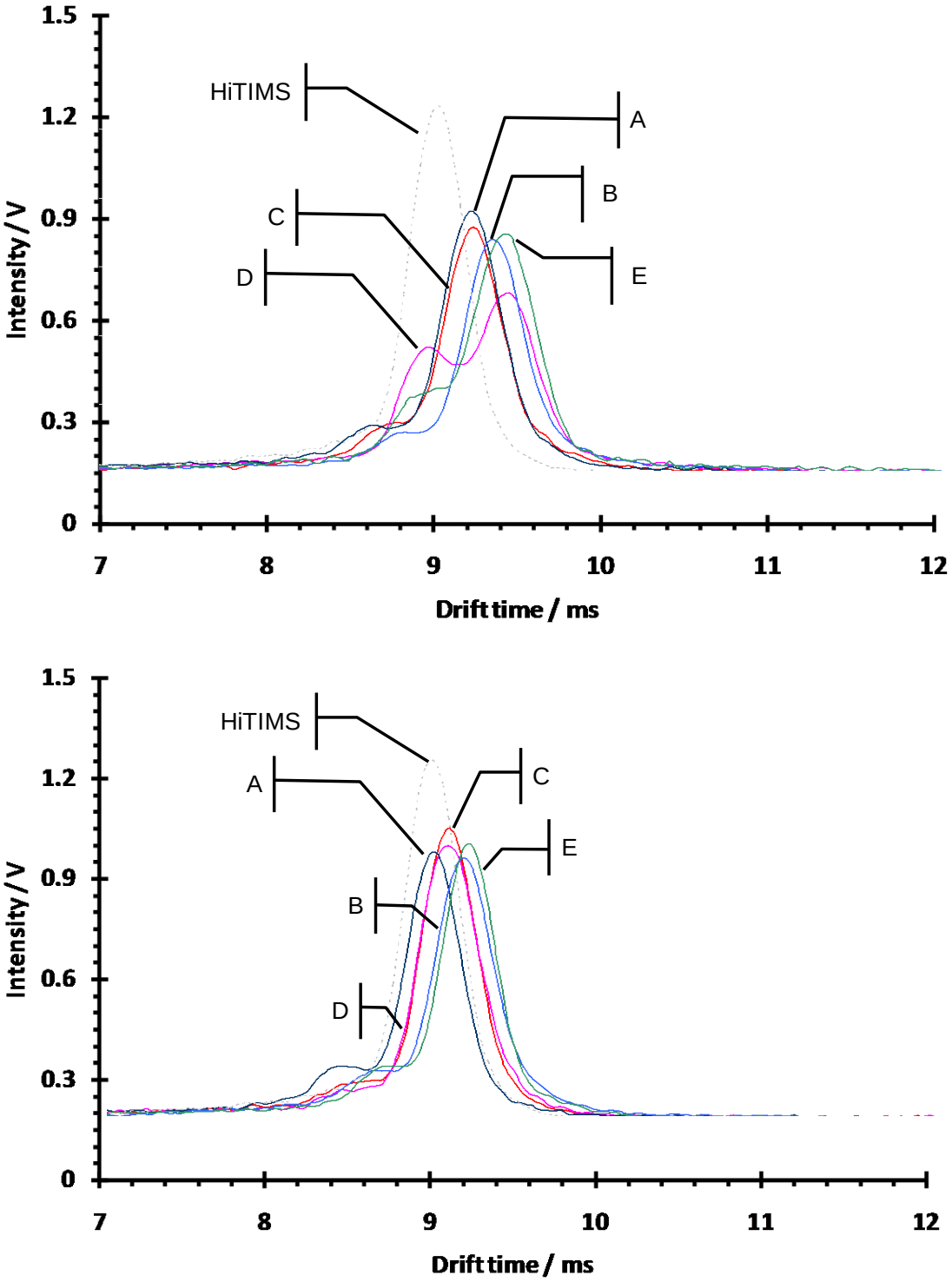

Figure 3 The effect of out-gassing products on the HTIMS response released from unconditioned (Top) and conditioned (Bottom) polymers at room temperature. Note that no other product ions were detected, A; Zeonor; B: Conductive polystyrene C: Zeonex D: Nylon; E: conductive nylon;

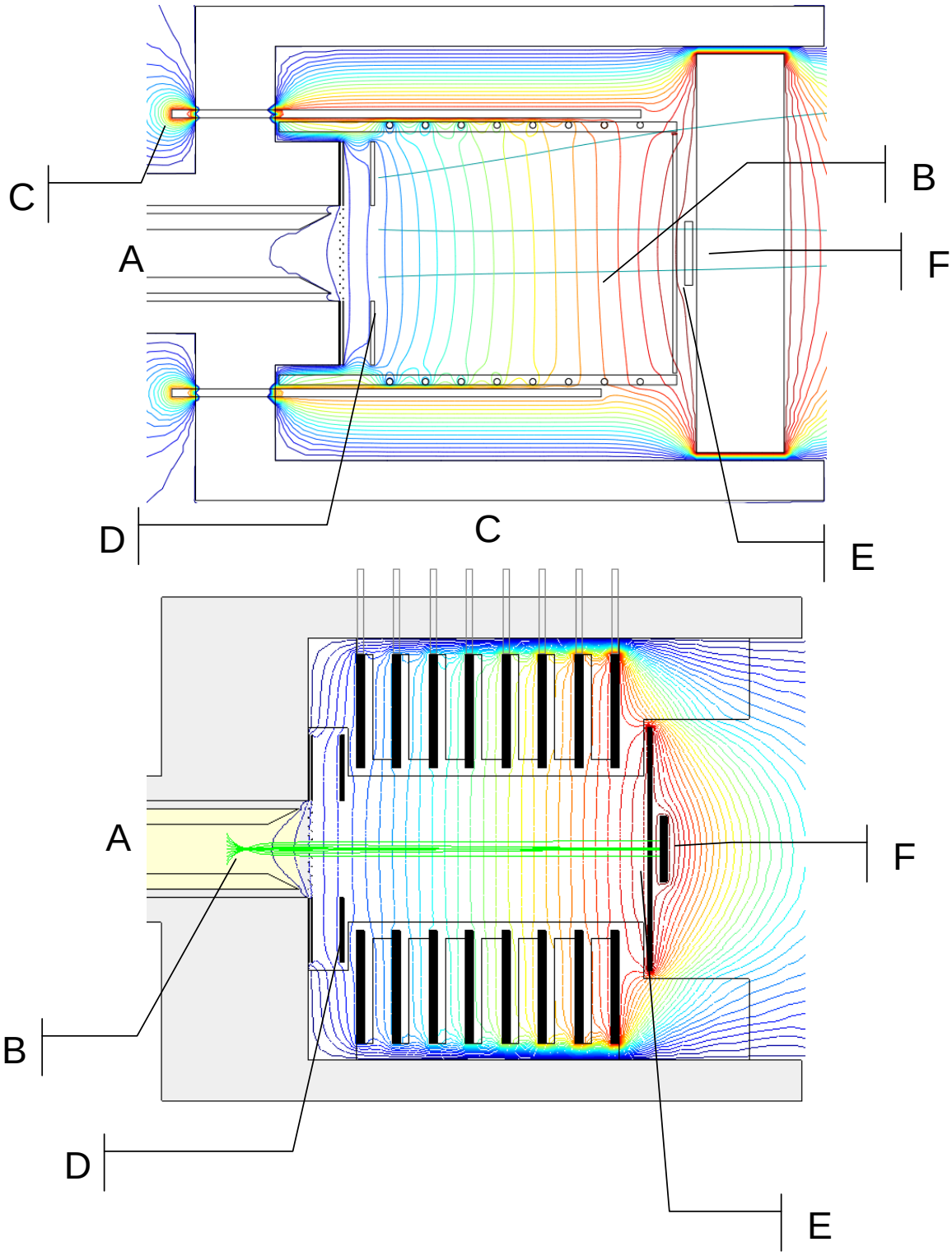

Figure 4 A comparison of the electric field models of the HiTIMS (Top), and the polymer snap together tube (bottom). Key, A: inlet; B: ion trajectories; C: voltage supplies to field defining electrodes; D: shutter grid assembly; E: shield grid; F: Faraday detector.

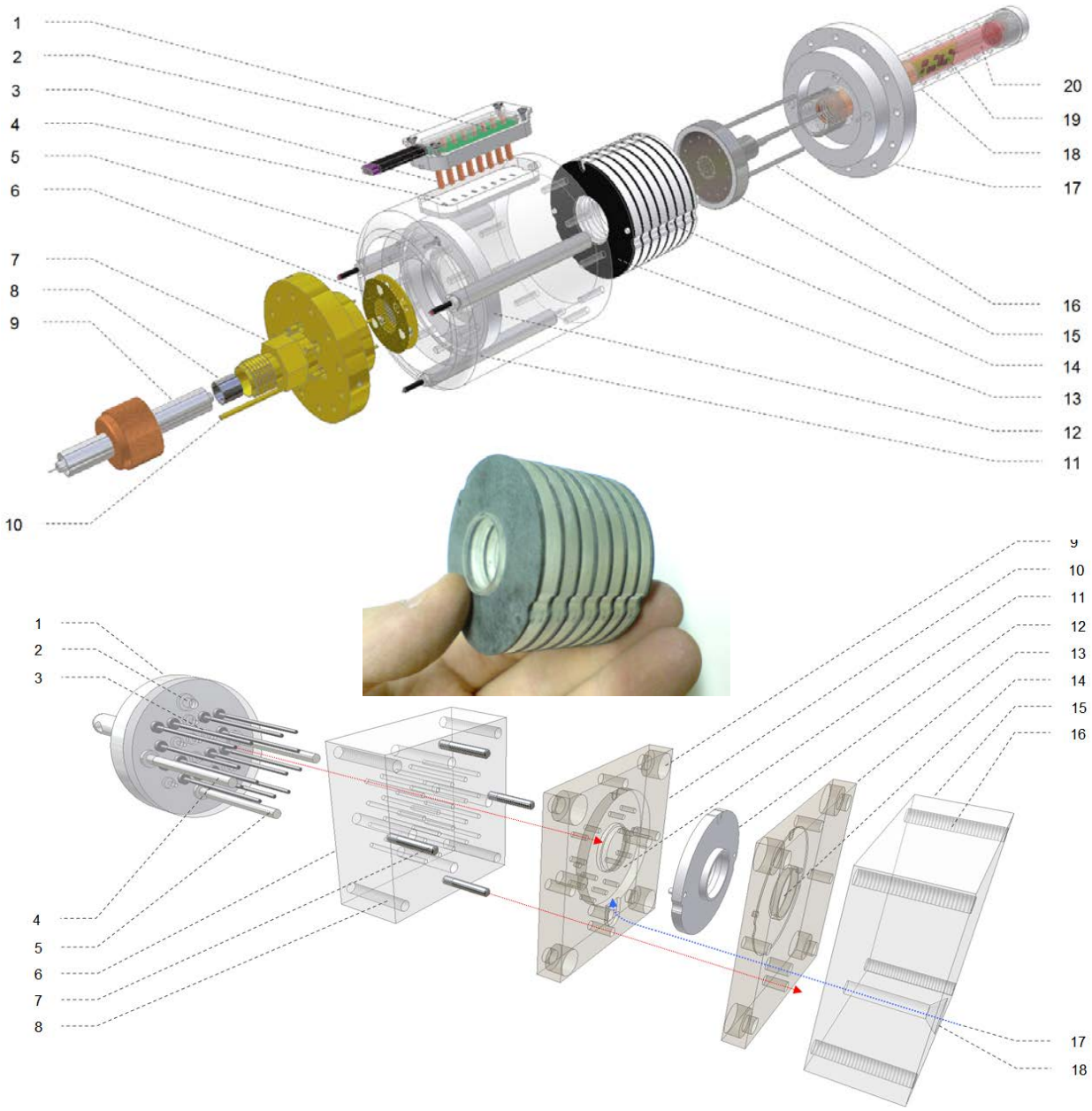

Figure 5. Exploded diagrams of: the ion mobility spectrometer assembly (Top); the injection molding tool assembly, for the encapsulating insulator (Bottom); and, a photograph showing the assembled drift tube (Middle).

Key to Figure 5.

Top. 1) PCB connector for voltage supply pins. 2) Injection molded voltage supply connector plug. 3) Stainless-steel “snap-fit” connector pins. 4) PTFE Voltage supply socket. 5) Aluminium housing and electrical shield (transparent view). 6) Ion shutters. 7) Graseby HTIMS inlet assembly manifold (includes item 6). 8) 63Ni ionisation source. 9) Sheath flow sample inlet. 10) Auxiliary exhaust port . 11) Cartridge heater. 12) Machined PTFE insulating holder to hold and align drift within the assembly. 13) Injection molded electrically conductive electrode. 14) Injection molded insulating spacer.15) Graseby HTIMS detector and drift flow gas inlet assembly. 16) Drift gas inlet. 17) Machined PTFE lid. 18) Machined and ventilated PTFE insulation. 19) Preamplifier printed circuit board. 20) Preamplifier electrical shielding, copper tube standing at 1.1kV (transparent view).

Bottom. 1) Steel ejector piston. 2) Empty pocked driver pin holder. 3) Ejector pin, these pins “punch” the molded part out of the mold cavity at the end of each cycle. The pins can move through the moving platform block and the moving mold to reach the deepest surface level of the part cavity in (11). 4) Guide pin. 5) Sprue ejector pin (4mm shorter than an ejector pin). 6) Moving platform, a steel block with holes for the various “pins” including dowel pin pockets. This part supports the “moving mold” (11) by the use of four 6mm bolts (not shown). 7) Dowel pin for the accurate alignment of the mold pair and the moving platform, illustrated by a red arrow. 8) Threaded hole for 6mm mold-fastener bolt. 9) Counter-bore clearance for the 6mm mold-fastener bolt. 10) Moving mold. 11) Moving mold part cavity, which carries a negative impression of the left side of the molded part shown in (12). 12) Injection molded part. 13) Fixed mold. 14) Fixed mold part cavity, which carries a negative impression of the right side of the molded part shown in (12). 15) Fixed platform with the polymer injection port and channel. This also supports the fixed mold with four 6mm bolts. 16) Threaded hole for 6mm mold-fastener bolt. 17) The blue arrow indicates the flow path of molten polymer through to the part cavity. 18) Polymer injection port.

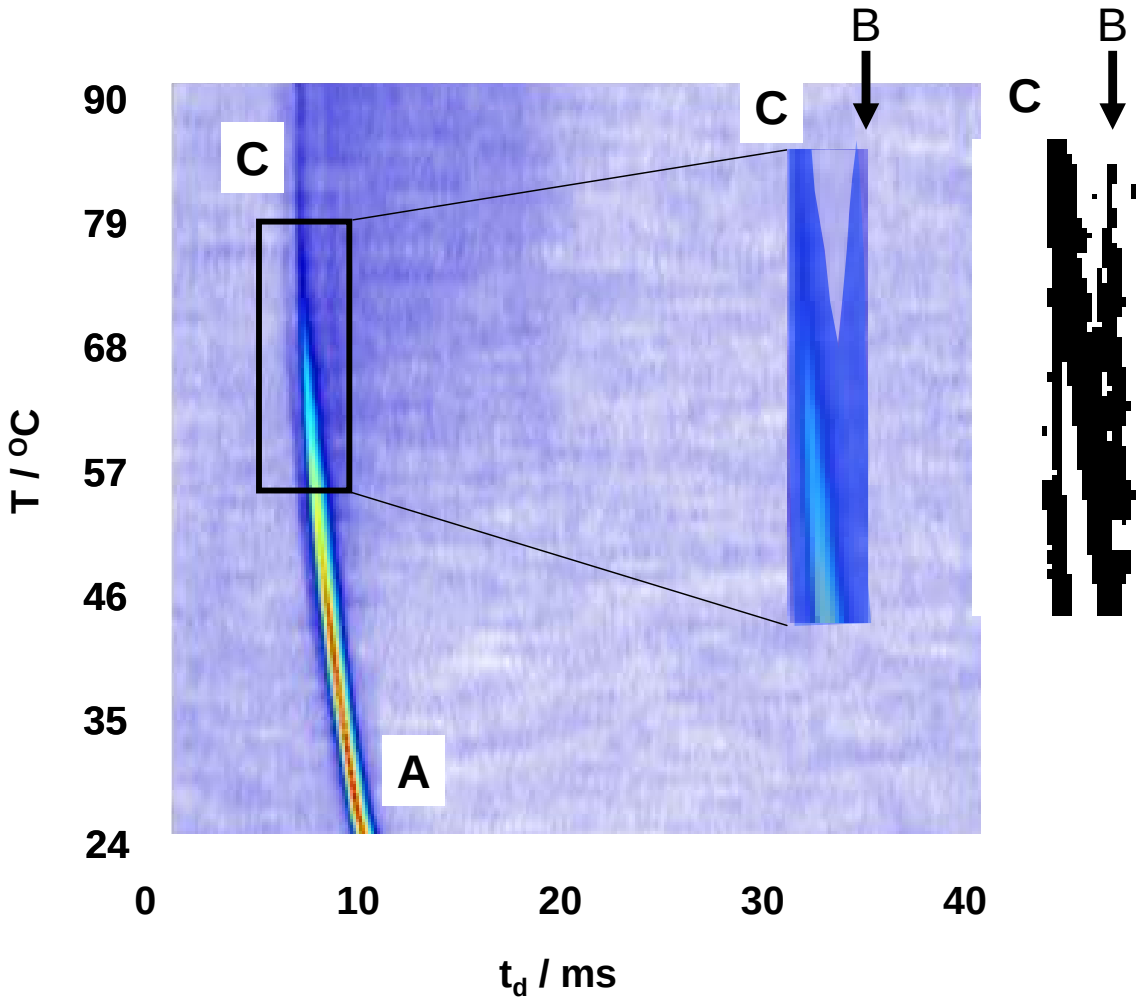

Figure 6. A false color image showing the intensity of the peaks in the temperature response surface for the Zeonex and conducting nylon polymeric drift tube. The inserts are enlargements, and enhancements, of the area of the surface where temperature driven modification of the polymer became pronounced, and the water based reactant ion peak was suppressed as the out-gassed ammonia started to dominate the reactant ion peak chemistry.

Key: A: shows the reactant ion water-based peak shift towards lower drift times with increasing temperature; B: traces of the original water-based reactant ion at temperatures above 50°C; and C, the development of what is thought to be an ammonia-based entity, accompanied by other out-gassed components arising from thermal decomposition.

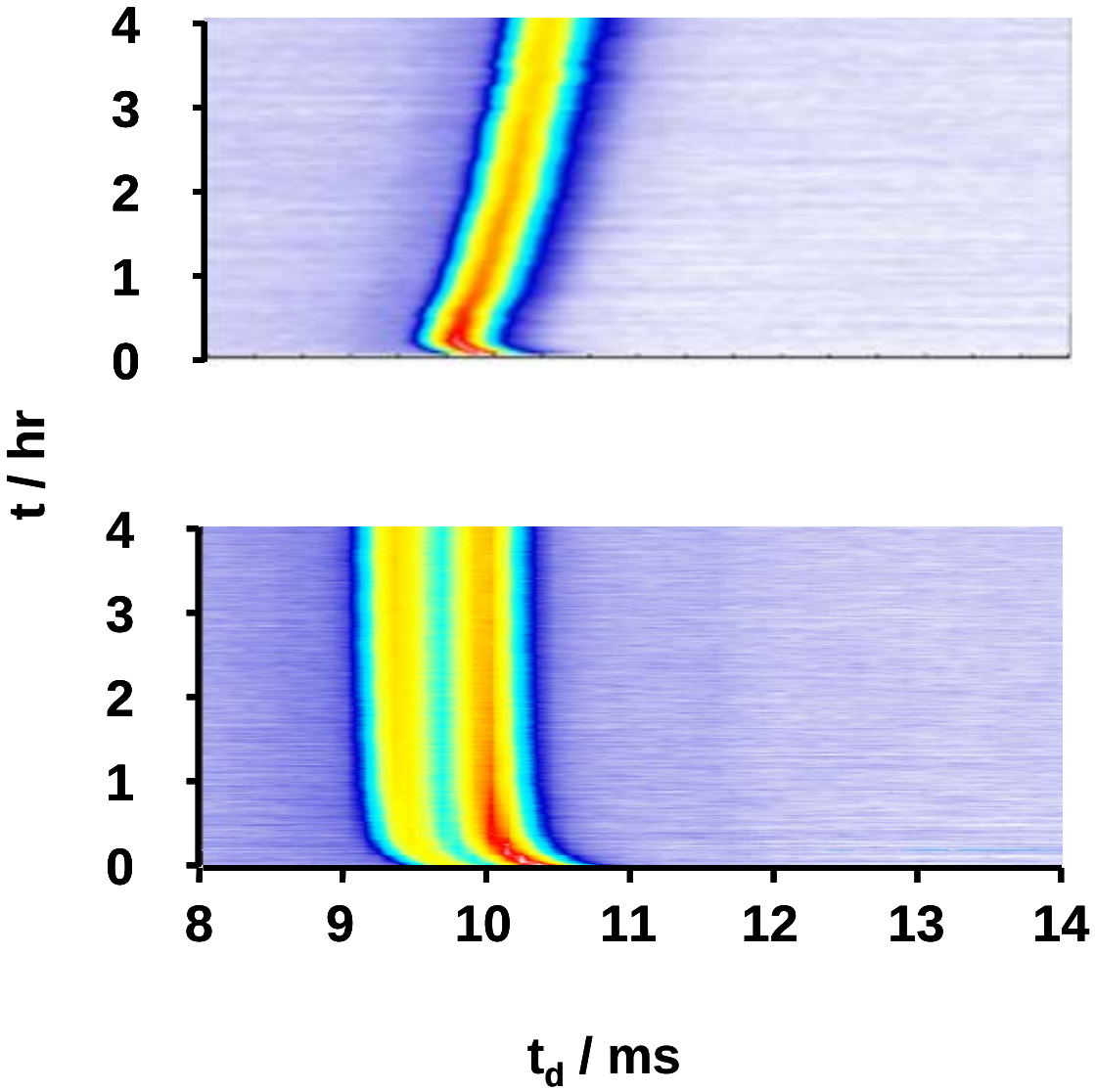

Figure 7. Summary of the stability tests for a combination of conductive Nylon field defining electrodes encapsulated in Zeonex (Top), and the same electrodes encapsulated in Nylon (Bottom). The loss of water from the electrodes and the associated reduction in drift times are evident in both sets of traces. The Nylon encapsulation yields ammonium-based ions from out-gassed products (td = 9.5 ms) while the high surface resistively of the Zeonex results in a reversible charge accumulation on the surface of the drift tube resulting in a suppression of the ion transfer efficiency of the drift tube and a gradual reduction in field strength leading to longer drift times.

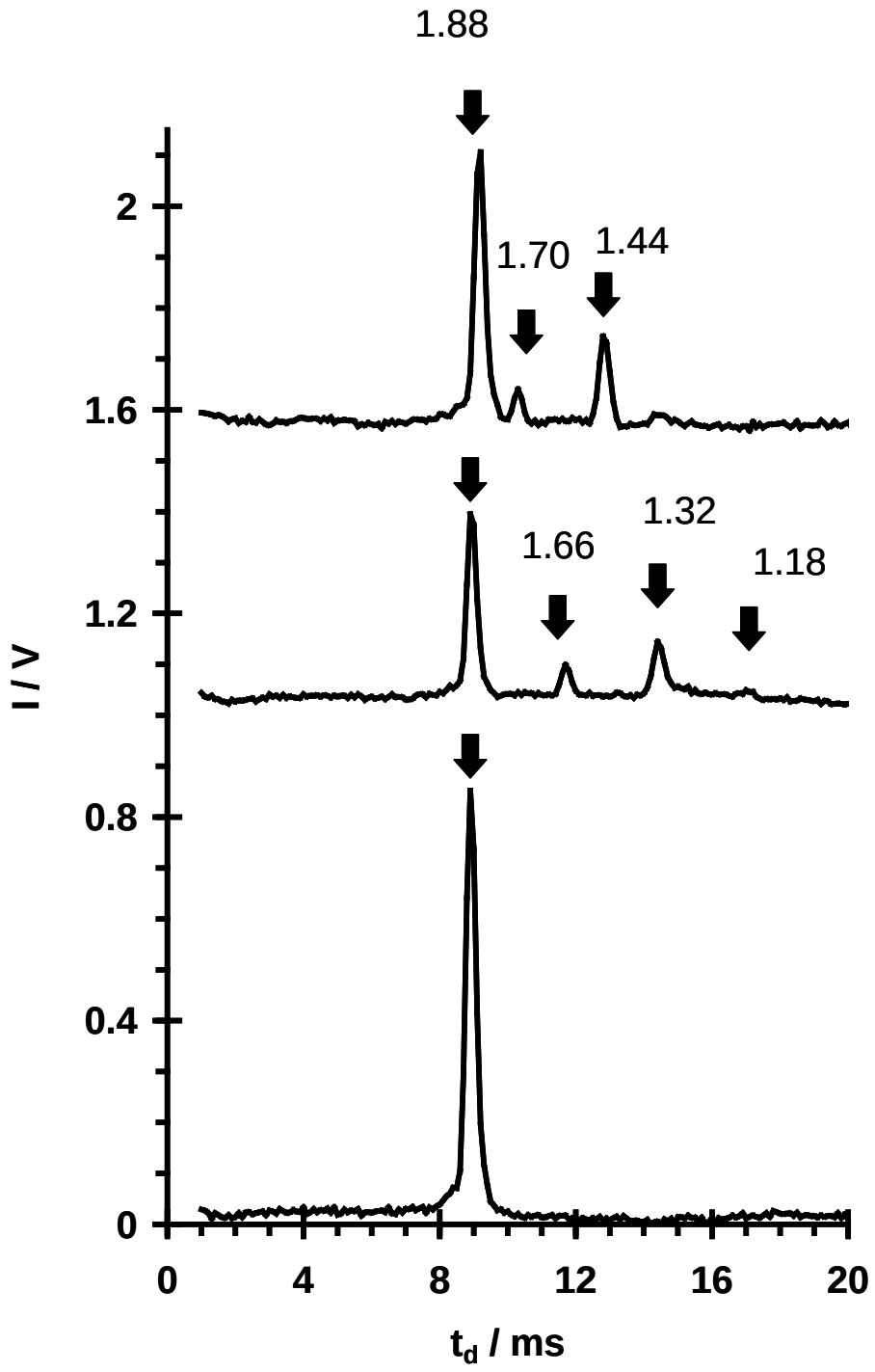

Figure 8. Example ion mobility spectra obtained for dimethylmethylphosphonate (2 ppm(v)) , top; and, hexan-1-ol (2ppm(v)), middle compared against a blank spectra. The data were collected at 22 °C using a conditioned and stabilised polymer drift tube with carbon loaded field defining electrodes encapsulated in Zeonex. The sheath-flow inlet was adjusted to regulate the mass-flux of analyte into the reactant region to generate these spectra. The numbers give the reduced mobilities of the product ions observed (cm2 V-1 s-1).

TABLES

Table 1. Summary of the five polymers examined in this study.

Material	T_D / °C	T_M / °C	Comment
Nylon	140	155	
Carbon-loaded Nylon	180	200	
Carbon-loaded polystyrene	90	105	
Zeonex	140	155	Cycloolefinpolymer (COP)
Zeonor	90	105	Norbornene-ethene copolymer,

Note: **T_D is the degassing temperature, T_M is the melting point.**

Table 2. Summary of instrument parameters used in the GC-MS headspace analysis of the five candidate polymers.

Thermal desorber		
Primary desorption flow	50	$cm^3\ min^{-1}$
Primary split		Splitless
Primary desorption temperature	180	˚C
Primary desorption time	5	min
Cold trap volume	19	µl
Cold trap temperature	-10˚	C
Cold trap packing		Tenax TA/Carbograph 1TD
Secondary desorption flow	1	$cm^3\ min^{-1}$
Secondary split	50:1	
Trap heating rate	100	˚C min^{-1}
Secondary desorption temperature	300	˚C
Secondary desorption time	3	min
Gas Chromatograph		
Column flow	1	$cm^3\ min^{-1}$
Initial column temperature	40	°C
Initial hold time	1	min
Column heating rate	10	°C min^{-1}
Final Column temperature	200	°C
Final hold time	20	min
Ion Trap Mass Spectrometer		
Ionisation EI mode	10	µA
Scan range	30 to 400	m/z
Scan time	1	S
Trap temperature	200	°C
Manifold Temperature	90	°C
Transfer line temperature	260	°C
Filament and Multiplier delay	30	µS

Table 3. Summary of the experimental conditions used in the out-gassing characterization tests.

Parameter		
Gas	**High purity nitrogen**	
Drift gas flow	**200**	**cm^3 min^{-1}**
Sheath gas flow	**70**	**cm^3 min^{-1}**
Sample carrier gas flow	**10**	**cm^3 min^{-1}**
IMS Cell		**HITIMS**
IMS Inlet temperature	**100**	**°C**
Drift cell temperature	**30**	**°C**
Drift gas temperature	**27**	**°C**
Averaged spectra	**60**	
Sampling rate	**10**	**kHz**
Gate pulse width	**0.3**	**ms**
Drift time measurement from:		**Ion gate closure**

Table 4. Summary of the effect of out gassing on the ammonium ($[(H_2O)_nH]^+$) and water ($[(H_2O)_n(NH_4)_m\ H]^+$) responses from a HiTIMS challenged with the headspace of 3 g of unconditioned (U) or conditioned (C) polymer.

Polymer	$[(H_2O)_nH]^+$				$[(H_2O)_n(NH_4)_m\ H]^+$			
	$K / cm^2\ V^{-1}\ s^{-1}$		I / V		$K / cm^2\ V^{-1}\ s^{-1}$		I / V	
	U	C	U	C	U	C	U	C
Blank-reference	1.88	1.88	1.09	1.05	2.00	2.01	0.09	0.10
Nylon	1.79	1.86	0.53	0.80	1.89	2.00	0.36	0.09
C-loaded nylon	1.80	1.83	0.71	0.81	1.91	1.95	0.23	0.16
C-loaded ^{o}PS	1.81	1.84	0.69	0.77	1.92	1.96	0.68	0.15
Zeonex	1.83	1.88	0.72	0.85	1.95	2.00	0.12	0.11
Zeonor	1.84	1.86	0.78	0.79	1.96	2.00	0.14	0.16